ChemComm

Digital Light Processing (DLP) 3D Printing of Polymer Networks Comprising Virus-like Particles

Journal:	*ChemComm*
Manuscript ID	CC-COM-05-2024-002411.R1
Article Type:	Communication

Data will be provided upon reasonable request. Please contact the corresponding authors:

Nicole Steinmetz: nsteinmetz@ucsd.edu
Alshakim Nelson: alshakim@uw.edu

ChemComm

COMMUNICATION

Digital Light Processing (DLP) 3D Printing of Polymer Networks Comprising Virus-like Particles†

Received 00th January 20xx,
Accepted 00th January 20xx

DOI: 10.1039/x0xx00000x

Naroa Sadaba[a §], Jorge Leganes Bayon[b,e-f §], Alshakim Nelson[a*], and Nicole F. Steinmetz[b-h*]

In this work, we introduce a 3D-printable virus-like particle (VLP)-enhanced cross-linked biopolymer system. VLPs displaying surface-available acrylate groups were prepared through aza-Michael addition to serve as resins. The VLP resins were then photopolymerized into a poly(ethylene glycol) diacrylate (PEGDA) network following DLP 3D printing. This approach represents a convergence of disciplines, where the synergistic interaction between virology and additive manufacturing unlocks new frontiers in biotechnology.

Additive manufacturing (or 3D printing) is a transformative technology with an immense potential to impact a broad array of sectors, such as automotive[1], aerospace[2], and medicine[3–5]. Digital light processing (DLP) 3D printing is a form of additive manufacturing in which light is used to sequentially pattern liquid resins into 3D constructs with exceptional detail and surface finish[6–8]. In general, the design of resins suitable for DLP 3D printing requires a low viscosity and a rapid rate of photocuring[9–11]. The most widely applied chemistry is that of free radical polymerization of acrylates or radical-initiated thiol-ene chemistry[12–16], due to their rapid rates of curing upon exposure to light. Thus, DLP 3D printing processes afford chemically cross-linked polymer networks (thermosets) as the product.

While resins for vat photopolymerization must be optimized for its printability and resolution of printed features, the cross-linked polymer network determines the mechanical properties of the printed construct. Therefore, the identification of resins that improve mechanical characteristics while maintaining printability are important to meet the future demands of the field. Herein, we demonstrate 3D-printed polymer networks with chemically incorporated virus-like particles (VLPs) to enhance a crosslinked polymer scaffold. VLPs from plant viruses serve as a platform nanotechnology with broad applications in medicine and materials[17–19]. The integration of VLPs into materials has been realized through hot-melt extrusion[20], electrospinning[21], as well as self-assembly[22]. In fact, VLPs have also been integrated into crosslinked polymers as fillers to enhance the mechanical and rheological properties of the materials[23,24]. However, their fabrication is limited by the tooling and setup used during nanocomposite design, which until now has restricted the applicability of these virus-based materials to laboratory settings[25]. In the present work, we not only incorporated VLPs into materials, rather we used the VLP as a printable bioink for additive manufacturing. Our approach could thus enable custom fabrication of VLP-based devices that can be directly translated into medical care, in fields such as tissue engineering and cancer immunotherapy. For example, VLP cancer vaccines could be realized into single-dose reservoirs[26] specifically designed for custom implantation into patients, facilitating treatment of tumors that cannot be accessible through intratumoral injection.

We chose the VLPs from physalis mottle virus (PhMV), a ~30 nm icosahedral plant virus with T = 3 symmetry comprising 180 identical ~21 kDa coat protein (CP) subunits[27]. PhMV offers a good stability profile[28] and is a versatile platform for functionalization through bioconjugate chemistry with addressable surface amino acids, cysteine on the interior and lysine on the exterior, for appending cargo (e.g. therapeutic molecules[29]) or linkers for integration into materials, as is demonstrated here. To utilize the VLPs as inks we functionalized the exterior lysine side chains with acrylate groups through aza-Michael addition and then photopolymerized the VLPs into a poly(ethylene glycol) diacrylate (PEGDA) network. Previous reports with bovine serum albumin have shown that PEGDA can react with surface amines to afford resins for 3D printing[30]. Here we expand these concepts to larger biomacromolecules, namely VLPs.

[a.] *Department of Chemistry, University of Washington, Seattle, WA 98195, USA*
[b.] *Aiiso Yufeng Li Family Department of Chemical and Nano Engineering, University of California San Diego, 9500 Gilman Dr., La Jolla, California 92093, United States*
[c.] *Department of Bioengineering, University of California San Diego, 9500 Gilman Dr., La Jolla, California 92093, United States*
[d.] *Department of Radiology, University of California San Diego, 9500 Gilman Dr., La Jolla, California 92093, United States*
[e.] *Center for Nano-ImmunoEngineering, University of California San Diego, 9500 Gilman Dr., La Jolla, California 92093, United States*
[f.] *Shu and K.C. Chien and Peter Farrell Collaboratory, University of California San Diego, 9500 Gilman Dr., La Jolla, California 92093, United States*
[g.] *Center for Engineering in Cancer, Institute of Engineering in Medicine, University of California San Diego, 9500 Gilman Dr., La Jolla, California 92093, United States*
[h.] *Moores Cancer Center, University of California, University of California San Diego, 9500 Gilman Dr., La Jolla, California 92093, United States.*
†Electronic Supplementary Information (ESI) available: experimental details, additional TGA and rheometric data. See DOI: 10.1039/x0xx00000x
§ These authors contributed equally

Using thermal analysis, tensile tests and rheometry, we characterized the thermal and mechanical properties of the 3D imprinted materials as a function of VLP incorporation.

The VLPs were expressed in and purified from *E. coli* using our established protocols[29]. VLPs were isolated at a yield of ~ 100 mg/L culture and stored in PBS buffer pH 7.2 at 4°C and characterized using a combination of electrophoresis techniques, size exclusion chromatography (SEC) and dynamic light scattering (DLS). To enable photopolymerization of the VLPs into the polymer networks, we first appended an acrylate handle by mixing PEGDA with the VLPs using molar excesses of 144x10^3-144x10^4 or 200-2000 equivalents of PEGDA per Lys side chains (the VLPs have 4 addressable Lys per CP or 720 Lys per VLP[31]). Under these conditions, PEGDA reacts with the VLPs via the aza-Michael addition to afford the VLP resins (VLP-R) (Figure 1A). The resins consist of a viscous liquid mixture of excess PEGDA (19.0-19.9 wt%), modified VLP-R (0.1-1.0 wt%) and DMSO (12 wt%) in PBS buffer. We prepared three resins of VLP-R-X, where X denotes the weight percentage of the VLP in the resin formulation, namely, 0.1, 0.5 and 1.0 wt% (Figure 1B).

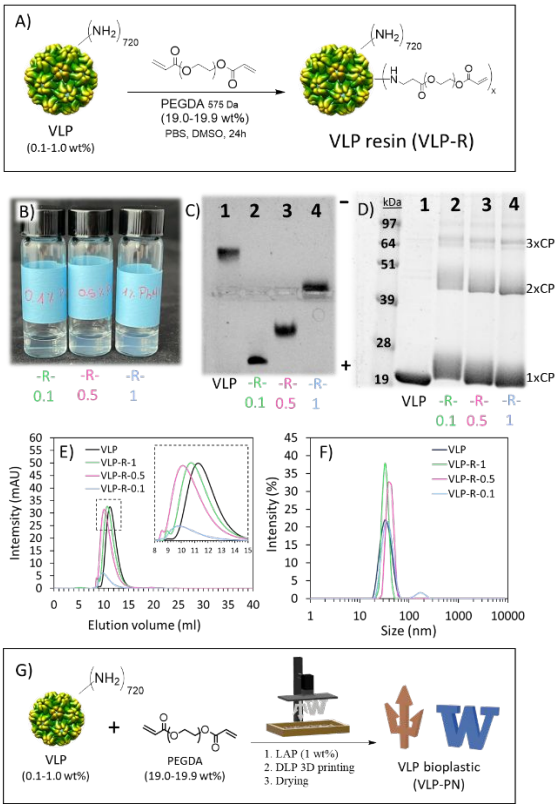

Figure 1. A) Scheme of the VLP resin (VLP-R) synthesis B) VLP resin formulations C) native electrophoresis D) SDS-PAGE E) Size-exclusion chromatography F) DLS analysis. G) Scheme of DLP 3D printing of the VLP bioplastics (VLP-PN).

To confirm successful VLP functionalization, the VLPs were first ultracentrifuged (121, 139 g, 70 min, 4°C, over a 20% sucrose cushion) to remove excess unreacted PEGDA. VLP-R were then characterized using native gel electrophoresis (Figure 1C). The un-modified PhMV VLPs (Lane 1) are positively charged,[31] and therefore migrate towards the cathode (-). On the contrary, VLP-R (Lanes 2-4) migrate towards the anode (+) due to the overall decrease in positive zeta charge as a result of PEGDA conjugation. While PEGDA is not a charged molecule, conjugation leads to a decreased number of primary amines on the VLP surface and hence decreased positive charge. The electrophoretic mobility toward the cathode is thus a function of degree of modification, the more PEGDA is reacted the faster the migration toward the cathode with VLP-R-0.1 (8000 eq/CP) > VLP-R-0.5 (1600 eq/CP) > VLP-R-1 (800 eq/CP). In that same order, we observed an increase in molecular weight of the virus CPs as shown in denaturing gel electrophoresis (Figure 1D, Lane 2-4), which is consistent with increasing degrees of PEGDA functionalization with increasing PEGDA equivalents. Moreover, a small fraction of CP dimers (~ 42 kDa, 5.5% total CP) and trimers (~ 64 kDa, 1.5% CP) was observed for all resin formulations, which indicates intraparticle crosslinking. Finally, size exclusion chromatography (SEC) of the VLPs (Figure 1E) revealed increasingly lower elution volumes for VLP and the resins VLP-R-1, 0.5 and 0.1, respectively, indicating a step-wise increase in size as a function of degree of labeling/excess used: VLP (0 eq/CP) < VLP-R-1 (800 eq/CP) < VLP-R-0.5 (1600 eq/CP) < VLP-R-0.1 (8000 eq/CP) which correlates larger particle size with increasing PEGDA functionalization and is consistent with electrophoretic data. DLS (Figure 1F) further indicates that monodisperse particles with no aggregation and hydrodynamic radii in the range of R_H = 32.7-43.8 nm with moderate polydispersity index (PDI) (see Table S1) were formulated.

Figure 1G shows the scheme for the fabrication of the VLP polymer networks (VLP-PN). Lithium phenyl-2,4,6-trimethylbenzoyl phosphinate (LAP) was added (1 wt%) to the aqueous resin as a photoinitiator. A commercial DLP 3D printer was used to fabricate 3D objects comprising the VLP-polymer networks. Because these were aqueous-based resins, the printed constructs were water-swollen hydrogels. Thus, the samples were dried overnight to obtain the VLP-PN. Three VLP-polymer networks were prepared and will be referred to as follows: VLP-PN-Y, wherein Y represents the weight percentage of the VLP (0.5, 2.5 or 5.0 wt%) in the non-hydrated polymer network (see Fig. S1).

Thermogravimetric analysis (TGA) was performed to study the thermal decomposition of the bioplastics. Figure 2A shows the thermograms of all samples. The native PEGDA polymer network (PEGDA-PN) and VLP-PN had similar profiles, with an initial onset of mass loss at 100 °C attributed to water loss (30 wt% and 24 wt% for PEGDA-PN and VLP-PNs, respectively) and a second more pronounced transition at 390 °C attributed the PEG backbone (60% wt% and 65% wt% for PEGDA PN and VLP-PNs, respectively). The incorporation of VLPs into the polymer networks increased the thermal stability of the VLP-PN plastics in the range of 200-400°C and, to a lesser extent, in the range of 400-1000°C (Figure 2A, inset). This gain in thermal stability in the VLP-PNs can be explained by the individual contributions in the thermal profiles of the native VLPs and neat PEGDA-PN (see Fig. S2). Almost throughout the entire temperature range, native VLPs are thermally more stable than neat

PEGDA-PN, and thus incorporating the VLPs into PEGDA network results in thermal stabilization of the plastics to a certain extent.

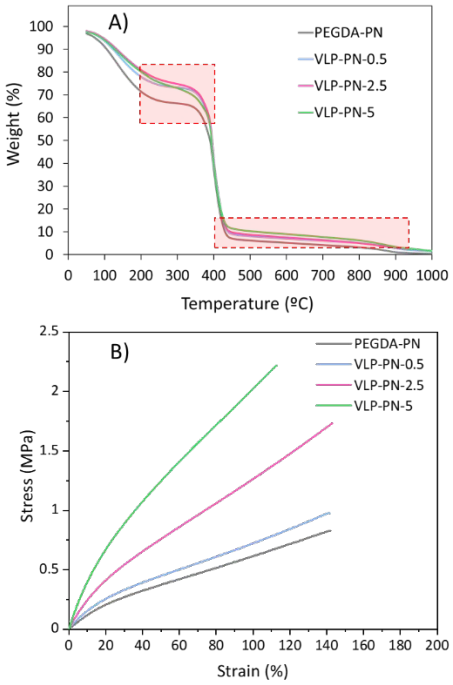

Figure 2. A) Thermograms of PEGDA and VLP bioplastics. PEGDA-PN refers to the bioplastic with 0 % wt VLPs and VLP-PN-0.5, VLP-PN-2.5 and VLP-PN-5 refer to the bioplastics with VLP weight contents of 0.5, 2.5 and 5.0 wt%, respectively. B) Stress-strain curve for VLP-PN samples (0.5-5%) and the native PEGDA network.

Next, tensile testing was conducted to assess the mechanical properties of VLP-PN as a function of VLP incorporation (Figure 2B). The data shows that the incorporation of VLPs enhances the mechanical characteristics of the PEGDA network, maintaining constant elongation but increasing the elastic modulus and toughness. Notably, VLP-PN-0.5 appears to maintain the properties of PEGDA-PN without significant alteration, likely due to the insufficient quantity of VLP particles added to the resin to manifest an improvement in mechanical properties. In contrast, both VLP-PN-2.5 and VLP-PN-5 exhibit a notable increase in both the modulus and ultimate strength of the material (Figure 2B, Table 1). Despite the lower degree of functionalization observed in the VLP-PN-2.5 and VLP-PN-5 resins with respect to VLP-PN-0.5 resin (see Figure 1), it is evident that this low level of functionalization can enhance the toughness of the material. Complete compositions of the formulations for the VLP resins and VLP bioplastics can be found in Tables S2 and S3.

Table 1. Mechanical properties for bioplastic formulation (VLP-PN-0.5, VLP-PN-2.5 and VLP-PN-5 with VLP weight contents of 0.5, 2.5 and 5.0 wt%, respectively) and neat PEGDA-PN (0 wt% VLP). E: elastic modulus, ε_u ultimate strain and U: Toughness, area under the curve.

Bioplastic	[PhMV] (wt%)	E (KPa)	ε_u (%)	U (Jm^{-3})
PEGDA-PN	0	1.2±0.01	145.30±3.0	0.69±0.03
VLP-PN-0.5	0.5	1.4±0.10	142.84±2.3	0.80±0.02
VLP-PN-2.5	2.5	2.4±0.04	130.90±10.3	1.21±0.10
VLP-PN-5	5	3.8±0.02	108.4±4.6	1.07±0.05

Following the material characterization, we proceeded with the optimization of the 3D printing process. Photorheometry was used for the initial assessment of curing times upon exposure to 365 nm light with an intensity of 20 mW/cm^2 (Fig. S3). All samples exhibited a rapid increase in the storage modulus upon irradiation with light, and a cross-over point between the storage and loss moduli was observed within 1 s of light exposure. Based on these experiments, the burn-in layer (the first printed layer attached to the build plate) was set to 0.5 s and subsequent layers were set to 0.3 s exposure times. To assess the resolution of printed objects, two computer-aided designs (CAD) were used: a square structure comprising etched lines of varying widths (1000, 500, 250, and 100 µm), and another structure to validate resolution further and ensure the absence of over-curing during printing, consisting of a rectangle with a 1 mm diameter hole (2 mm deep) and a 1 mm diameter cylinder (2 mm height). The analysis of Optical microscopy images (see Figure 3A) revealed that all structures achieved good resolution at 100 µm and did not exhibit signs of over-curing during the printing process[32,33].

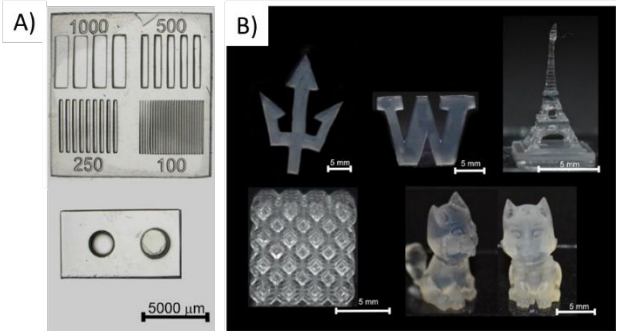

Figure 3. A) Optical microscope Image for 3D printing optimization and B) photos of SLA 3D Printing structures for VLP-PN-0.5.

Once the print resolution was confirmed, different objects were printed to showcase the versatility of DLP 3D printing. As shown in Figure 3B, all designs were printable with a good resolution and without overcuring.

In conclusion, we successfully demonstrated the surface of the VLPs can be efficiently functionalized with acrylate groups following aza-Michael addition with PEGDA crosslinker. This process enabled the formulation of VLP resins for DLP 3D printing of virus-polymer networks, wherein the virus enhanced the thermal stability and mechanical properties of the material. This method of processing customized 3D-printed virus materials opens new avenues in the fields of additive manufacturing, as well tissue engineering and cancer immunotherapy, with exquisite control over 3D form factors.

Acknowledgements

This work was supported This work was supported by the NSF Center for the Chemistry of Molecularly Optimized Networks (MONET), CHE-2116298. The authors acknowledge the use of facilities and instrumentation supported by NSF through the UC San Diego Materials Research Science and Engineering Center (UCSD MRSEC), grant DMR-2011924.

Data availability statement

Data will be provided upon reasonable request. Please contact the corresponding authors:

Nicole Steinmetz: nsteinmetz@ucsd.edu
Alshakim Nelson: alshakim@uw.edu

Conflicts of interest

There are no conflicts to declare.

Notes and references

1 Zareanshahraki, F.; Davenport, A.; Cramer, N.; Seubert, C.; Lee, E.; Cassoli, M.; Wang, X. 3D Print Addit Manuf, 2021, 8(5), 302-314
2 Lim, C. W. J.; Le, K. Q.; Lu, Q.; Wong, C. H. *IEEE Potentials* 2016, *35* (4), 18–22.
3 Xu, X.; Awad, A.; Robles-Martinez, P.; Gaisford, S.; Goyanes, A.; Basit, A. W. *Journal of Controlled Release* 2021, *329*, 168–3659.
4 Guttridge, C.; Shannon, A.; O'sullivan, A.; O'sullivan, K. J.; O'sullivan, L. W. Annals of 3D Printed Medicinem, 2022, 5, 100044
5 Bao, Y.; Paunović, N.; Leroux, J.-C.; Bao, Y.; Paunović, N.; Leroux, J.-C. *Adv Funct Mater* 2022, *32* (15), 2109864.
6 Shafique, H.; Karamzadeh, V.; Kim, G.; Shen, M. L.; Morocz, Y.; Sohrabi-Kashani, A.; Juncker, D. Lab Chip, 2024, 24, 2774.
7 Liz-Basteiro, P.; Sanz-Horta, R.; Reviriego, F.; Martínez-Campos, E.; Reinecke, H.; Elvira, C.; Rodríguez-Hernández, J.; Gallardo, A. Additive Manufacturing, 2023, 75, 103758
8 Zhang, J.; Hu, Q.; Wang, S.; Tao, J.; Gou, M. Int J Bioprint. 2020, 6(1), 242.
9 Sch, S.; Teixeira, S. M.; Feijen, J.; Grijpma, D. W.; Poot, A. A. Macromol Biosci, 2013, 13(12), 1711-9
10 Smith, P. T.; Altin, G.; Millik, S. C.; Narupai, B.; Sietz, C.; Park, J. O.; Nelson, *ACS Appl. Mater. Interfaces* 2022, *14*.
11 Yu, S.; Sadaba, N.; Sanchez-Rexach, E.; Hilburg, S. L.; Pozzo, L. D.; Altin-Yavuzarslan, G.; Liz-Marzán, L. M.; Jimenez De Aberasturi, D.; Sardon, H.; Nelson, A. Adv. Funct. Mater. 2023, 33, 2300332.
12 Maines, E. M.; Porwal, M. K.; Ellison, C. J.; Reineke, T. M. *Green Chemistry*. 2021, 23 (18), 6863–6897.
13 Yu, C.; Schimelman, J.; Wang, P.; Miller, K. L.; Ma, X.; You, S.; Guan, J.; Sun, B.; Zhu, W.; Chen, S. Chem Rev, 2020, 120(19), 10695-10743
14 Ligon, S. C.; Liska, R.; Rgen Stampfl, J.; Gurr, M.; Mü, R.; Fuller, ‖ H B. Chem Rev. 2017, 117(15), 10212-10290
15 Bobrin, V. A.; Lee, K.; Zhang, J.; Corrigan, N.; Boyer, C.; Bobrin, V. A.; Lee, K.; Corrigan, N.; Boyer, C.; Zhang, J. Adv Mater 2022, 34(4), e2107643
16 Cosola, A.; Chiappone, A.; Sangermano, M. *Mol. Syst. Des. Eng* 2022, *7*, 1093.
17 Hun Chung, Y.; Church, D.; Koellhoffer, E. C.; Osota, E.; Shukla, S.; Rybicki, E. P.; Pokorski, J. K.; Steinmetz, N. F. Nat Rev Mater, 2022, 7, 372–388.
18 Nam, K. T.; Kim, D. W.; Yoo, P. J.; Chiang, C. Y.; Meethong, N.; Hammond, P. T.; Chiang, Y. M.; Belcher, A. M. *Science,* 2006, *312* (5775), 885–888.
19 Dang, X.; Yi, H.; Ham, M.-H.; Qi, J.; Soo Yun, D.; Ladewski, R.; Strano, M. S.; Hammond, P. T.; Belcher, A. M. *NATURE NANOTECHNOLOGY,* 2011, *6*.
20 Lee, P. W.; Shukla, S.; Wallat, J. D.; Danda, C.; Steinmetz, N. F.; Maia, J.; Pokorski, J. K. *ACS Nano* 2017, *11*, 5.
21 Honarbakhsh, S.; Guenther, R. H.; Willoughby, J. A.; Lommel, S. A.; Pourdeyhimi, B.; Honarbakhsh, S.; Guenther, R. H.; Willoughby, A. Adv Healthc Mater. 2013, 2(7), 1001-7.
22 Kostiainen, M. A.; Hiekkataipale, P.; Laiho, A.; Lemieux, V.; Seitsonen, J.; Ruokolainen, J.; Ceci, P. Nat Nanotechnol, 2013, 8(1),52-6
23 Zheng, Y.; Dougherty, M. L.; Konkolewicz, D.; Steinmetz, N. F.; Pokorski, J. K. Polymer, 2018, 142, 72-79
24 Southan, A.; Lang, T.; Schweikert, M.; Tovar, G. E. M.; Wege, C.; Eiben, S.RSC Adv,2018, 8(9), 4686-4694.
25 Dickmeis, C.; Kauth, L.; Commandeur, U. Wiley Interdiscip Rev Nanomed Nanobiotechnol, 2021, 13(1), e1662
26 Ray, S.; Puente, A.; Steinmetz, N. F.; Pokorski, J. K. Wiley Interdiscip Rev Nanomed Nanobiotechnol, 2023, 15(1), e1832.
27 Barkovich, K. J.; Wu, Z.; Zhao, Z.; Simms, A.; Chang, E. Y.; Steinmetz, N. F. Bioconjug Chem, 2023, 34(9), 1585-1595
28 Wu, Z.; Bayón, J. L.; Kouznetsova, T. B.; Ouchi, T.; Barkovich, K. J.; Hsu, S. K.; Craig, S. L.; Steinmetz, N. F. Nano Lett. 2024, 24, 10, 2989–2997
29 Barkovich, K. J.; Zhao, Z.; Steinmetz, N. F. Small Sci. 2023, 3, 2300067
30 Sanchez-Rexach, E.; Smith, P. T.; Gomez-Lopez, A.; Fernandez, M.; Cortajarena, A. L.; Sardon, H.; Nelson, A.*ACS Appl Mater Interfaces,* 2021, *13* (16), 19193–19199.
31 Masarapu, H.; Patel, B. K.; Chariou, P. L.; Hu, H.; Gulati, N. M.; Carpenter, B. L.; Ghiladi, R. A.; Shukla, S.; Steinmetz, N. F. Biomacromolecules, 2017, 18(12), 4141-4153
32 Mathew, E.; Pitzanti, G.; Gomes Dos Santos, A. L.; Lamprou, D. A.. *Pharmaceutics* 2021, *13* (11), 1837.
33 Goodarzi Hosseinabadi, H.; Nieto, D.; Yousefinejad, A.; Fattel, H.; Ionov, L.; Miri, A. K. *Appl Mater Today* 2023, *30*, 101721.